Neovascularization of ischemic myocardium by human bone-marrow–derived angioblasts prevents cardiomyocyte apoptosis, reduces remodeling and improves cardiac function

A.A. KOCHER[1], M.D. SCHUSTER[1], M.J. SZABOLCS[3], S. TAKUMA[2], D. BURKHOFF[2], J. WANG[1], S. HOMMA[2], N.M. EDWARDS[1] & S. ITESCU[1,2]

Departments of Surgery[1], Medicine[2] and Pathology[3], Columbia University, New York, New York, USA
Correspondence should be addressed to S.I.; email: si5@columbia.edu

Left ventricular remodeling is a major cause of progressive heart failure and death after myocardial infarction. Although neoangiogenesis within the infarcted tissue is an integral component of the remodeling process, the capillary network is unable to support the greater demands of the hypertrophied myocardium, resulting in progressive loss of viable tissue, infarct extension and fibrous replacement. Here we show that bone marrow from adult humans contains endothelial precursors with phenotypic and functional characteristics of embryonic hemangioblasts, and that these can be used to directly induce new blood vessel formation in the infarct-bed (vasculogenesis) and proliferation of preexisting vasculature (angiogenesis) after experimental myocardial infarction. The neoangiogenesis resulted in decreased apoptosis of hypertrophied myocytes in the peri-infarct region, long-term salvage and survival of viable myocardium, reduction in collagen deposition and sustained improvement in cardiac function. The use of cytokine-mobilized autologous human bone-marrow–derived angioblasts for revascularization of infarcted myocardium (alone or in conjunction with currently used therapies) has the potential to significantly reduce morbidity and mortality associated with left ventricular remodeling.

Although prompt reperfusion within a narrow time window has significantly reduced early mortality from acute myocardial infarction, post-infarction heart failure resulting from ventricular remodeling is reaching epidemic proportions[1]. The remodeling process is characterized by progressive expansion of the initial infarct area and dilation of the left ventricular lumen[2,3], with cardiomyocyte replacement by fibrous tissue deposition in the ventricular wall[4–6]. One approach proposed to reverse myocardial remodeling is regeneration of cardiac myocytes using bone-marrow–derived mesenchymal stem cells[7,8]. Such multipotent cells have been identified in adult-human bone marrow, do not express hematopoietic lineage markers such as CD34 or CD45 and can be induced under appropriate culture conditions to differentiate into lineages of diverse mesenchymal tissues such as bone, cartilage, fat, tendon and both skeletal and cardiac muscle[9]. Cardiomyocyte differentiation and improvement in myocardial function requires *in vitro* culture with 5-azacytidine[7,10].

Another integral component of the remodeling process is the development of neoangiogenesis within the myocardial infarct scar[11,12], a process requiring activation of latent collagenase and other proteinases[13]. Under normal circumstances, the contribution of neoangiogenesis to the infarct-bed capillary network is insufficient to keep pace with the tissue growth required for contractile compensation and is unable to support the greater demands of the hypertrophied but viable myocardium. The relative lack of oxygen and nutrients to the hypertrophied myocytes might be an important etiological factor in the death of otherwise viable myocardium, resulting in progressive infarct extension and fibrous replacement. Because late reperfusion of the infarct vascular bed in both humans and animal models significantly benefits ventricular remodeling and survival[14–16], we postulated that augmentation of vascular-bed neoangiogenesis might improve cardiac function by preventing loss of hypertrophied but otherwise viable cardiac myocytes.

Bone-marrow–derived elements have the potential to induce therapeutic angiogenesis of ischemic tissues[17–20]; however, the precise nature of such endothelial precursors is not known[21–23]. In the prenatal period, hemangioblasts derived from the human ventral aorta give rise to cellular elements involved in both vasculogenesis and hematopoiesis[24,25]. In addition to hematopoietic lineage markers, embryonic hemangioblasts are characterized by expression of the vascular endothelial cell growth factor receptor-2 (VEGFR-2) and have high proliferative potential with blast colony formation in response to VEGF (refs. 26–29). The earliest precursor of both hematopoietic and endothelial cell lineages to have diverged from embryonic ventral endothelium has been shown to express VEGF receptors as well as α_4-integrins and the transcription factor GATA-2, which is required for differentiation of embryonic hemangioblasts to pluripotent stem cells[30,31]. Here we show that endothelial cell precursors are present in adult-human bone marrow and have properties of hemangioblasts. We also show that they can be mobilized, expanded and used to induce both vasculogenesis and angiogenesis, thus protecting hypertrophied myocytes against apoptosis and preventing remodeling and heart failure after experimental myocardial infarction.

G-CSF mobilizes hematopoietic and mesenchymal lineage cells

Following treatment with granulocyte-colony stimulating factor (G-CSF), we collected mobilized mononuclear cells and separated them into two fractions using a monoclonal antibody against CD34 coupled to magnetic beads. In the $CD34^+$ fraction (> 98% purity),

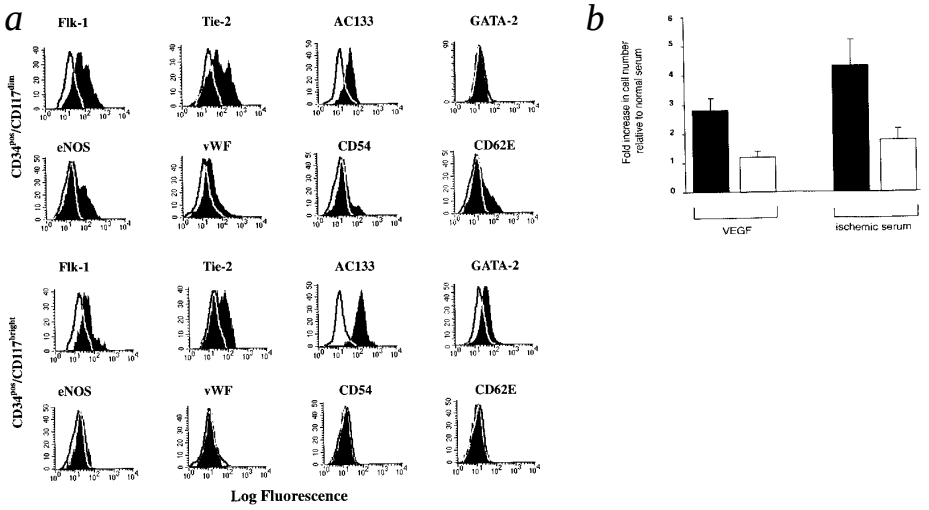

Fig. 1 G-CSF mobilizes into the circulation a human bone-marrow–derived population which differentiates into endothelial cells. ***a***, Four-parameter flow cytometric phenotypic characterization of living (defined by 7-AAD staining), G-CSF–mobilized cells derived from adult-human bone marrow. For each marker used, shaded areas represent background log fluorescence relative to isotype control antibody. ***b***, Proliferative responses to various stimuli of single-donor $CD34^+$ human cells sorted on the basis of bright and dim CD117 expression and co-expression of intracellular GATA-2 protein. Graph shows 96-h proliferative responses. ■, $CD117^{Bright}/GATA\text{-}2^{Hi}$; □, $CD117^{Dim}/GATA\text{-}2^{Lo}$ ($P < 0.01$ for both comparisons).

90–95% co-expressed the hematopoietic lineage marker CD45, 60–80% co-expressed the stem-cell–factor receptor CD117 and less than 1% co-expressed the monocyte/macrophage lineage marker CD14. In contrast, the $CD34^-$ fraction contained 15–30% monocyte/macrophage lineage cells co-expressing CD14 and CD45 and 30–40% non-hematopoietic lineage cells ($CD45^-$). Within the latter fraction, 10–15% of cells co-expressed CD29, CD44 and CD90, markers characteristic of bone-marrow–derived mesenchymal cells[9].

Mobilized $CD34^+$ cells contain endothelial cells and angioblasts

Among double-positive $CD34^+/CD117^+$ cells, CD117 expression was dim in 75–85% and bright in 15–25%. Both $CD34^+/CD117^{Dim}$ and $CD34^+/CD117^{Bright}$ populations contained cells of endothelial lineage, as defined by expression of VEGFR-2 (Flk-1) (Fig. 1*a*). VEGFR-2 expression was detected at high density on 20–30% of $CD117^{Dim}$ cells and at lower density on 10–15% of $CD117^{Bright}$ cells. By quadruple parameter analysis, the VEGFR-2^+ cells within the $CD34^+/CD117^{Dim}$ population displayed phenotypic characteristics of mature vascular endothelia, including high level expression of Tie-2, eNOS, vWF, E-selectin (CD62E) and ICAM (CD54). In contrast, the VEGFR-2^+ cells within the $CD34^+/CD117^{Bright}$ subset displayed phenotypic characteristics of endothelial progenitors, including co-expression of Tie-2, as well as AC133 (ref. 32), but not eNOS, vWF, E-selectin and ICAM. In addition, we showed that these cells express proteins characteristic of primitive hemangioblasts arising during waves of murine and human embryogenesis, including the transcription factors GATA-2 and GATA-3. Intracellular staining of $CD34^+$ cells sorted on the basis of CD117 bright or dim expression demonstrated that GATA-2 protein levels, as determined by mean channel fluorescence, were approximately 25% higher in the $CD34^+/CD117^{Bright}$ than in the $CD34^+/CD117^{Dim}$ population. We confirmed this by quantitative mRNA measurement, with GATA-2 mRNA levels found to be 58% higher in $CD34^+$ cells expressing $CD117^{Bright}$ compared with those expressing $CD117^{Dim}$. Because we also detected surface expression of VEGFR-2, Tie-2, and AC133 on a subset of $CD34^+/CD117^{Dim}$ cells that had low levels of GATA-2

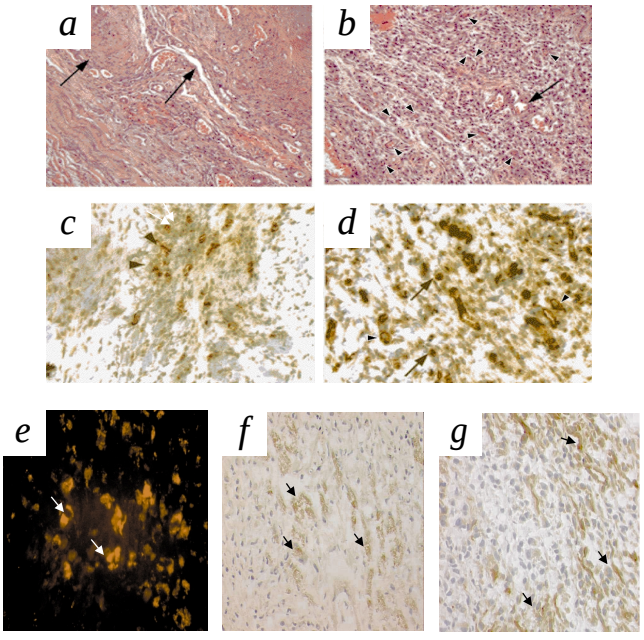

Fig. 2 Injection of G-CSF–mobilized human $CD34^+$ cells into rats with acute myocardial infarction induces neoangiogenesis involving endothelium of both human and rat origin at 2 wk post-LAD ligation. ***a***, H&E-stained infarct zone of control rat injected with saline shows a myocardial scar composed of paucicellular, dense fibrous tissue (arrows; magnification: ×200). ***b***, H&E-stained infarct zone of rat injected with human $CD34^+$ cells shows significant increase in microvascularity and cellularity of granulation tissue, numerous capillaries (arrowheads), feeding vessels (arrow) and decrease in matrix deposition and fibrosis (magnification: ×200). ***c***, Anti–factor-VIII immunohistochemic staining of ischemic myocardium from rat injected with saline shows only focal areas of granulation tissue with factor-$VIII^+$ vascularity and interstitial cells (arrowheads) and diffuse increase in matrix deposition (arrows; magnification: ×400). ***d***, Anti–factor-VIII immunohistochemic staining of ischemic myocardium from rat injected with human $CD34^+$ cells demonstrates diffuse increase in factor-$VIII^+$ capillaries (arrowheads), and in factor-$VIII^+$ interstitial cells, (arrows; magnification: ×400). ***e–g***, Immunophenotypic characterization of the species origin of capillaries in infarcted rat myocardium. *e*, Endothelial cells lining numerous capillaries (arrows) within myocardial infarct bed demonstrate DiI fluorescence 2 wk after intravenous injection of DiI-labeled human $CD34^+$ cells. *f*, In consecutive sections, the human origin of these endothelial cells in the central infarct zone is confirmed by immunohistochemical staining using anti-human CD31 mAb (arrows). *g*, In consecutive sections, endothelium lining numerous other blood vessels are of rat origin (arrows), as confirmed by immunohistochemic staining using anti-rat CD31 mAb, and lack of human CD31 or DiI expression.

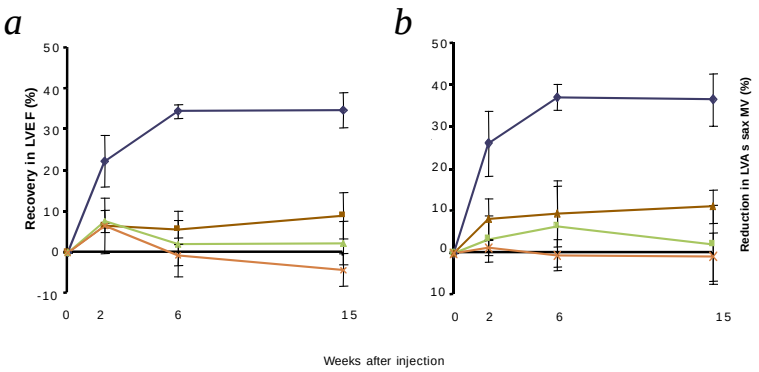

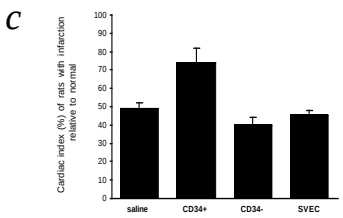

Fig. 3 Injection of G-CSF–mobilized human CD34⁺ cells into rats with acute infarction improves myocardial function. ***a*** and ***b***, Effects G-CSF–mobilized human CD34⁺ (> 98% purity) cells, CD34⁻ (< 2% purity) cells, peripheral SVEC or saline injected intravenously 48 h after myocardial infarction, on the function of rat hearts over a 15-wk period. Only injections of G-CSF–mobilized adult-human CD34⁺ cells was accompanied by significant, sustained LVEF recovery (*a*; $P < 0.001$) and reduction in LVAs (*b*; $P < 0.001$). In *a* and *b*: blue ◆, CD34+ cells; maroon ■, CD34– cells; green ▲, SVEC; orange X, saline. ***c***, At 15 wk post-infarction, rats injected with CD34⁺ cells showed significantly less reduction in mean cardiac index relative to normal rats compared with each of the other groups ($P < 0.001$).

mRNA and protein activity (data not shown), we conclude that identification of an embryonic bone-marrow–derived angioblast phenotype requires concomitant CD117^{Bright} surface expression and cellular GATA-2 activity in addition to expression of VEGFR-2, Tie-2 and AC133.

Properties of angioblasts cultured *in vitro*

Because the frequency of circulating endothelial cell precursors in animal models has been shown to be increased by either VEGF (ref. 33) or regional ischemia[17–20], we next examined the proliferative responses of phenotypically-defined angioblasts to VEGF and to factors in ischemic serum. CD117^{Bright}/GATA-2^{Hi} angioblasts demonstrated significantly higher proliferative responses relative to CD117^{Dim}/GATA-2^{Lo} bone-marrow–derived cells from the same donor following culture for 96 h with either VEGF or ischemic serum (both $P < 0.01$; Fig. 1*b*). The expanded angioblast population consisted of large blast cells, defined by forward scatter, which continued to express immature markers, including GATA-2, GATA-3 and CD117^{Bright}, but not markers of mature endothelial cells, including eNOS or E-selectin (data not shown). This indicates blast proliferation without differentiation under these culture conditions. However, culture on fibronectin with endothelial growth medium resulted in outgrowth of monolayers with endothelial morphology as well as functional and phenotypic features characteristic of endothelial cells, including uniform uptake of acetylated LDL, and co-expression of CD34, CD31 and factor VIII (data not shown). Thus, G-CSF treatment of adult humans mobilizes a bone-marrow–derived population with phenotypic and functional characteristics of embryonic angioblasts, as defined by specific surface phenotype, high proliferative responses to VEGF and cytokines in ischemic serum and ability to differentiate into endothelial cells by culture in medium enriched with endothelial growth factors.

CD34⁺ cells induce cardiac vasculogenesis and angiogenesis

Intravenous injection of 2×10^6 freshly obtained, DiI-labeled human CD34⁺ cells (> 98% purity, containing both hematopoietic and endothelial progenitors) resulted in infiltration of the infarct zone within 48 h of LAD ligation, but this did not occur in unaffected myocardium or myocardium of sham-operated rats. Histologic examination at two weeks post-infarction revealed that injection of CD34⁺ cells was accompanied by a significant increase in infarct zone microvascularity, cellularity and numbers of factor-VIII⁺ angioblasts and capillaries, and was also accompanied by reduction in matrix deposition and fibrosis in comparison to controls (Fig. 2*a–d*). Neoangiogenesis was increased within both the infarct zone and the peri-infarct rim in rats receiving CD34⁺ cells compared with saline controls (mean numbers of factor-VIII⁺ capillaries per high power field for CD34⁺ cells versus saline treated groups, respectively, were: 247 ± 12 versus 52 ± 8 in the infarct zone, $P < 0.01$; 162 ± 9 versus 51 ± 5 in the peri-infarct rim, $P < 0.01$). We observed no increases in capillary numbers at sites distal to the infarct zone in rats injected with either CD34⁺ cells or saline (36 ± 2 versus 37 ± 3 capillaries per high power field). Capillaries of human origin, defined by endothelial cells co-expressing DiI fluorescence and human but not rat CD31 accounted for 20–25% of the total myocardial capillary vasculature after injection of CD34⁺ cells. These were located exclusively within the central infarct zone of collagen deposition (Fig. 2*e–g*). In contrast, capillaries of rat origin, as determined by expression of rat but not human CD31, demonstrated a distinctly dif-

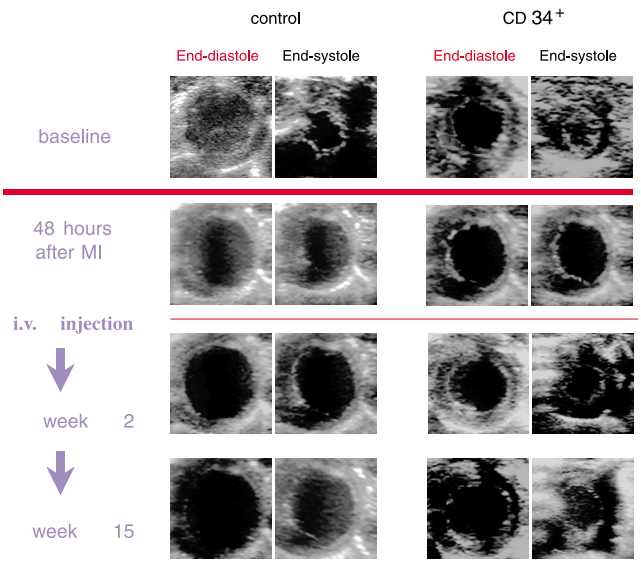

Fig. 4 Representative echocardiographic examples of rats undergoing LAD ligation and subsequently receiving saline (control) or human CD34⁺ cells intravenously. At 48 h after LAD ligation, systolic function is severely compromised in both rats. At 2 wk after injection, systolic function is improved only in the rat receiving CD34⁺ cells. This effect persists at 15 wk.

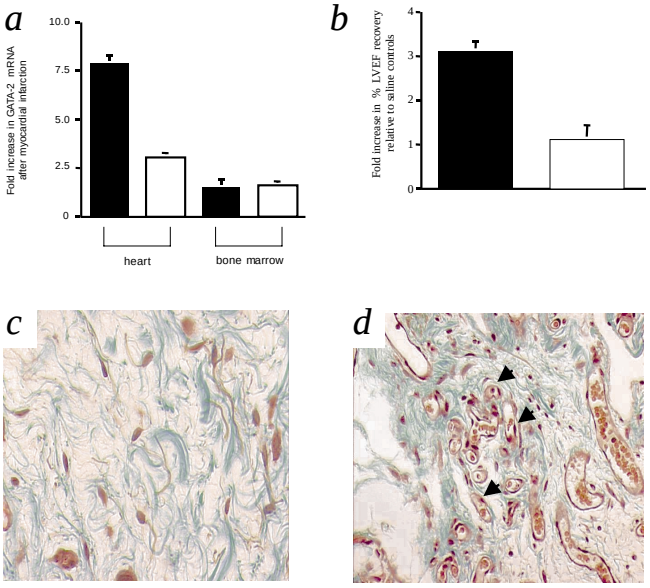

Fig. 5 Neoangiogenesis and improvement in myocardial function is dependent on angioblast population within human CD34$^+$/CD117^{Bright} subset. ***a***, Measurement of human GATA-2 mRNA expression in the bone marrow and heart of infarcted rats colleced at 48 h after receiving CD34$^+$ cells (■; > 98% purity) or CD34$^+$ cells (□; < 2% purity), normalized for total human RNA measured by GAPDH expression. GATA-2 mRNA in ischemic tissues is expressed as the fold increase relative to non-ischemic tissues. ***b***, Hearts of rats injected with CD34$^+$ cells containing both CD117^{Bright} and CD117^{Dim} cells (■) showed over 3-fold improvement at 2 wk in LVEF compared with hearts of rats receiving CD34$^+$/CD117^{Dim} cells alone (□) (expressed as mean fold improvement ± s.e.m. relative to saline controls). ***c*** and ***d***, Infarct zones of rats injected with CD34$^+$ cells containing both CD117^{Bright} and CD117^{Dim} cells (*d*) showed 3–5-fold higher capillary numbers (arrowheads) at 2 wk compared with rats receiving CD34$^+$/CD117^{Dim} cells alone (*c*).

ferent pattern of localization. These were absent within the central zone of collagen deposition and abundant both at the peri-infarct rim between the region of collagen deposition and myocytes and between myocytes. Although intravenous injection of CD34$^-$ cells (< 2% CD34 purity, containing monocyte/macrophage lineage cells and mesenchymal progenitors) or saphenous vein endothelial cells (SVEC) resulted in similar degrees of infiltration of ischemic rat myocardium as CD34$^+$ cells, neither induced an increase in capillary numbers (data not shown).

Myocardial function improved by CD34$^+$ cells

We next compared the effects of injecting four cellular fractions on myocardial function of rats following infarction. After LAD ligation, left ventricular ejection fraction (LVEF) decreased by means of 25–43% and left ventricular end-systolic area (LVAS) increased by means of 44–90%. Remarkably, by two weeks after injection of G-CSF–mobilized adult-human CD34$^+$ lineage cells, and in a parallel time-frame with the observed neoangiogenesis, LVEF recovered by a mean of 22 ± 6% ($P < 0.001$; Fig. 3*a*). This effect was long-lived, with LVEF recovering by a mean of 34 ± 4% at 15 weeks after injection. Similarly, CD34$^+$ cells reduced LVAS by a mean of 26 ± 8% by 2 weeks and 37 ± 6% by 15 weeks ($P < 0.001$; Fig. 3*b*). Neither CD34$^-$ mesenchymal precursors nor any other group demonstrated similar effects. At 15 weeks post-infarction, mean cardiac index in rats injected with CD34$^+$ cells was only reduced by 26 ± 8% relative to normal rats, whereas for each of the other groups it was reduced by 48–59% ($P < 0.001$; Fig. 3*c*). Fig. 4 shows representative echocardiographic images for each group.

Angioblasts required for neoangiogenesis

We next performed a series of experiments designed to show that the GATA-2^{Hi}CD117^{Bright} fraction within the bone-marrow–derived CD34$^+$ population contains cells with functional angioblast activity necessary for the observed neo-angiogenesis. At 48 h following ischemia induced by LAD ligation, human GATA-2 mRNA expression in rat myocardium was almost three-fold higher after injection of CD34$^+$ cells compared with CD34$^-$ cells (Fig. 5*a*). In contrast, human GATA-2 mRNA expression in rat bone marrow was similar for both groups, indicating that a GATA-2$^+$ population within CD34$^+$ adult-human bone-marrow–derived cells selectively migrates to myocardium following induction of ischemia. Infarct zones of rats injected with CD34$^+$ cells containing both CD117^{Bright} and CD117^{Dim} cells demonstrated 3–5-fold higher capillary numbers at two weeks compared with infarct zones of rats receiving CD34$^+$/CD117^{Dim} cells alone (Fig. 5*c* and *d*). Moreover, hearts of rats injected with CD34$^+$ cells containing both CD117^{Bright} and CD117^{Dim} cells demonstrated over three-fold higher improvement in LVEF at two weeks compared with hearts of rats receiving CD34$^+$/CD117^{Dim} cells alone (Fig. 5*b*). Together, these data indicate that injection of CD34$^+$ cells with phenotypic features of mature endothelium is not sufficient for induction of neoangiogenesis in ischemic tissues, and suggest that co-administration of a CD34$^+$/CD117^{Bright}/GATA-2^{Hi} population is a necessary requisite.

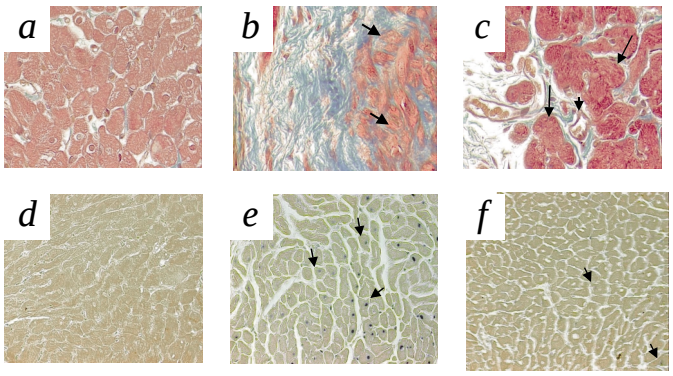

Fig. 6 Neoangiogenesis accompanying injection of human CD34$^+$ lineage cells protects hypertrophied myocardial cells against apoptosis. ***a–c***, Trichrome stain of normal (*a*), infarcted rat myocardium at 2 wk after injection of saline (*b*) or human CD34$^+$ cells (*c*). After saline injection, the myocytes in the peri-infarct rim were small, had irregular shape and a distorted appearance (arrows). In contrast, after CD34$^+$ cell injection, myocytes in the peri-infarct rim were large, regularly oval shaped (arrows) and surrounded by blood vessels (arrowhead). Magnification: ×40. ***d–f***, Concomitant staining of normal (*d*) and infarcted rat myocardium (*e* and *f*) with anti-desmin mAb and TUNEL assay to identify apoptotic myocytes with intranuclear DNA fragmentation. After injection of saline (*e*), the small, irregularly-shaped myocytes at the peri-infarct rim had the highest index of apoptotic nuclei. Few apoptotic myocytes are evident in the peri-infarct rim of rats receiving C34$^+$ cells (arrows) (*f*). Magnification: ×20.

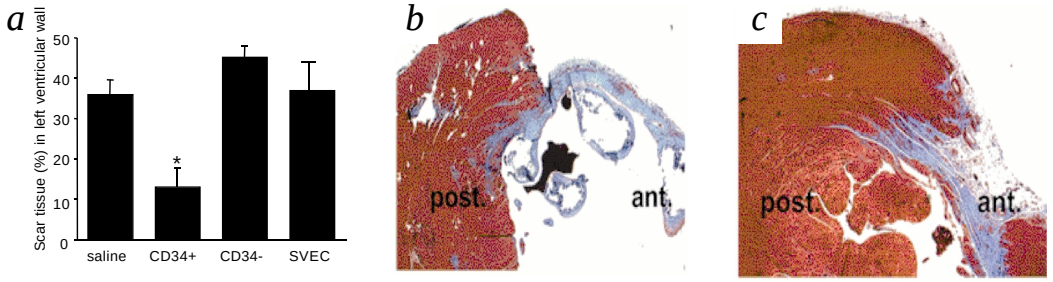

Fig. 7 Injection of G-CSF–mobilized human CD34⁺ cells into rats with acute infarction modifies the process of myocardial remodeling. ***a***, Between-group differences in percent scar:normal left ventricular tissue at 15 wk. (*P< 0.01, compared with each of the other groups). ***b***, Trichrome stain of rat myocardium at 15 wk post-infarction in rat injected with saline. The collagen-rich myocardial scar in the anterior wall of the left ventricle ('ant.') stains blue and viable myocardium stains red. Focal islands of collagen deposition (blue) are also present in the posterior wall of the left ventricle ('post.'). There is extensive loss of anterior wall myocardial mass, with collagen deposition and scar formation extending almost through the entire left ventricular wall thickness. Magnification: ×25. ***c***, In contrast, trichrome stain of rat myocardium at 15 wk post-infarction in rat receiving highly purified CD34⁺ cells demonstrates significantly reduced infarct-zone size and increased mass of viable myocardium within the anterior wall (ant.). Numerous vessels are evident at the junction of the infarct zone and viable myocardium. There is no focal collagen deposition in the left ventricular posterior wall (post.). Magnification: ×25.

Neoangiogenesis prevents apoptosis of hypertrophied myocytes

We next sought to determine the mechanism by which induction of neoangiogenesis resulted in improved cardiac function. Two weeks after LAD ligation the myocytes in the peri-infarct rim of saline controls had a distorted, irregular shape and a decreased diameter similar to myocytes from rats without infarction (0.020 mm ± 0.002 versus 0.019 mm ± 0.001; Fig. 6*a–c*). In contrast, the myocytes at the peri-infarct rim of rats who received CD34⁺ cells had a regular ovular shape, and were significantly larger than myocytes from control rats (diameter: 0.036 mm ± 0.004 versus 0.019 mm ± 0.001, $P < 0.01$). By concomitant staining for the myocyte-specific marker desmin and DNA end-labeling, six-fold lower numbers of apoptotic myocytes were detected in infarcted left ventricles of rats injected with CD34⁺ cells compared with saline controls (apoptotic index 1.2 ± 0.6 versus 7.1 ± 0.7, $P < 0.01$; Fig. 6*d–f*). These differences were particularly evident within the peri-infarct rim, where the small, irregularly shaped myocytes in the saline-treated controls had the highest index of apoptotic nuclei. In addition, whereas apoptotic myocytes extended throughout 75–80% of the left ventricular wall in saline controls, apoptotic myocytes were only detectable for up to 20–25% of the left ventricle distal to the infarct zone in rats injected with CD34⁺ cells. Together, these results indicate that the infarct zone vasculogenesis and peri-infarct angiogenesis induced by injection of CD34⁺ cells prevented a radially extending pro-apoptotic process evident in saline controls, which enabled survival of hypertrophied myocytes within the peri-infarct zone and improved myocardial function.

Early neoangiogenesis prevents late myocardial remodeling

With the last series of experiments, we sought to relate the degree of peri-infarct rim myocyte apoptosis at two weeks in control and experimental groups (saline versus CD34⁺ cells) with progressive myocardial remodeling over the ensuing four months. Despite similar initial reductions in LVEF and increases in LVAS, by two weeks the mean proportion of collagenous deposition or scar tissue/normal left ventricular myocardium (as defined by Masson's trichrome stain) was 3% in rats receiving CD34⁺ cells compared with 12% for those receiving saline. By 15 weeks post-infarction, the mean proportion of scar:normal left ventricular myocardium was 13% in rats receiving CD34⁺ cells compared with 36–45% for each of the other groups studied (saline, CD34⁻ and SVEC, $P < 0.01$; Fig. 7*a*). Rats receiving CD34⁺ cells demonstrated significantly increased mass of viable myocardium within the anterior free wall (Fig. 7*b* and *c*), which comprised myocytes exclusively of rat origin, expressing rat but not human major histocompatibility markers (data not shown). This confirmed intrinsic myocyte salvage rather than myocyte regeneration from human stem-cell precursors. Whereas collagen deposition and scar formation extended through almost the entire left ventricular wall thickness in controls (with aneurysmal dilatation and typical EKG abnormalities) the infarct scar extended only to 20–50% of the left ventricular wall thickness in rats receiving CD34⁺ cells. Moreover, pathological collagen deposition in the non-infarct zone was markedly reduced in rats receiving CD34⁺ cells. Together, these results strongly indicate that the reduction in peri-infarct myocyte apoptosis observed at two weeks resulted in prolonged survival of hypertrophied but viable myocytes and prevented myocardial replacement with collagen and fibrous tissue by 15 weeks.

Discussion

Following infarction, the viable myocardial tissue bordering the infarct zone is significantly hypertrophied[5,34,35]. Although neoangiogenesis within the infarcted tissue appears to be an integral component of the remodeling process[11,12], under normal circumstances the capillary network cannot keep pace with tissue growth and is unable to support the greater demands of the hypertrophied but viable myocardium which subsequently undergoes apoptosis due to inadequate oxygenation and nutrient supply[36,37]. Here we have demonstrated that an alternative approach, namely neoangiogenesis of the infarct bed by human bone-marrow–derived endothelial cell precursors, prevents apoptosis of hypertrophied but otherwise viable myocardium, reduces progressive collagen deposition and scar formation, and improves ventricular function in a rodent model of myocardial ischemia. The human endothelial precursors can be defined on the basis of specific surface phenotype, differentiating them from the mesenchymal lineage cardiomyocyte precursors, and enabling them to be used either alone or in combination with myocyte regeneration strategies or pharmacological therapies.

The development of neoangiogenesis within the myocardial infarct scar seems to require activation of latent collagenase and other proteinases following plasminogen activation by urokinase-type plasminogen activator (u-PA) expressed on infiltrating leukocytes[13]. The importance of bone-marrow–derived endothelial precursors in this process has been demonstrated in u-PA–deficient mice where transplantation of bone marrow from congenic wild-type strains restored defective myocardial revascularization post-infarction[13]. Expression and proteolytic activity of u-PA in human mononuclear cells and tumor cell lines are significantly increased by the colony

stimulating factors G-CSF, M-CSF, and GM-CSF (refs. 38–40); this provides a rationale for *in vivo* or *ex vivo* use of these cytokines to mobilize and differentiate large numbers of human adult bone-marrow–derived angioblasts for therapeutic revascularization of the infarct zone.

Our data indicate that cellular RNA and protein expression of the transcription factor GATA-2 can be used to selectively identify human adult bone-marrow–derived angioblasts capable of responding to signals from ischemic sites by proliferating and migrating to the infarct zone, and subsequently participating in the process of neoangiogenesis. Of particular interest, GATA-2 is a cofactor for endothelial cell transcription of preproendothelin-1 (ppET-1) (ref. 41), the precursor molecule of the potent vasoconstrictor and hypertrophic autocrine peptide ET-1. Transcription of ppET-1 is also increased by angiotensin II (ref. 42), produced as a result of activation of the renin-angiotensin neurohormonal axis following myocardial infarction. The angioblasts infiltrating the infarct bed may be secreting high levels of ET-1 due to the synergistic actions of angiotensin II surface receptor signaling and GATA-2 transactivation. Previous studies have shown that newly-formed vessels within the infarct bed have thicker walls, lower vasodilator responses and stronger vasoconstrictor responses to vasoactive substances than vessels within normal myocardium[43]. Our findings support the possibility that infarct bed neoangiogenic vasculature is derived from infiltrating GATA-2$^+$ angioblasts with increased autocrine ET-1 activity. The additional observation that proliferating capillaries at the peri-infarct rim and between myocytes were of rat origin indicates that in addition to vasculogenesis, human angioblasts or other co-administered bone-marrow–derived elements may be a rich source of pro-angiogenic factors, enabling additional induction of angiogenesis from pre-existing vasculature. The relative contribution of processes involving vasculogenesis or angiogenesis to the overall prevention of myocyte apoptosis remains to be precisely determined.

Together, the results of our study indicate that injection of G-CSF–mobilized adult-human CD34$^+$ cells with phenotypic and functional properties of embryonic hemangioblasts can stimulate neoangiogenesis in the infarct vascular bed, thus preventing myocyte apoptosis and reducing collagen deposition and scar formation after myocardial infarction. Although the degree of reduction in myocardial remodeling as a result of neoangiogenesis was striking, further augmentation in myocardial function might be achieved by combining infusion of human angioblasts with angiotensin-converting enzyme (ACE) inhibition or AT_1-receptor blockade to reduce angiotensin-II–dependent cardiac fibroblast proliferation, collagen secretion, and plasminogen activator-inhibitor (PAI) production[44,45]. The use of cytokine-mobilized autologous human bone-marrow–derived angioblasts for revascularization of myocardial infarct tissue, in conjunction with currently used therapies[46–48], offers the potential to significantly reduce morbidity and mortality associated with left ventricular remodeling post-myocardial infarction.

Methods

Purification and characterization of cytokine-mobilized human CD34$^+$ cells. Mononuclear cells were obtained from single-donor leukopheresis products of humans treated with recombinant G-CSF 10 μg/kg (Amgen, Thousand Oaks, California; s.c. incjection) daily for four d. Highly-purified CD34$^+$ cells (> 98% positive) were obtained using magnetic beads coated with monoclonal antibodies (mAb) against CD34 (Miltenyi Biotech, Placer County, California), stained with fluorescein-conjugated mAbs against CD34 and CD117 (Becton Dickinson, Franklin Lakes, New Jersey), VEGFR-2, Tie-2, vWF, eNOS (Santa Cruz Biotech, Santa Cruz, California), AC133 (Miltenyi Biotech, Placer County, California), CD54 (Immunotech, Boston, Massachusetts), CD62E (BioSource, Sunnyvale, California) and analyzed by four-parameter fluorescence using FACScan (Becton Dickinson). CD34$^+$ cells were also stained with PE-conjugated mAb against CD117 (Becton Dickinson), and sorted for functional studies on the basis of bright and dim fluorescence using a FACStar Plus (Becton Dickinson). Intracellular staining for GATA-2 was performed by permeabilizing one million cells from each of the brightly and dimly fluorescing cell populations using a Pharmingen Cytofix/Cytoperm kit, and incubating with fluorochrome-conjugated mAbs against CD117, CD34 and GATA-2 (Santa Cruz Biotech, Santa Cruz, California) or IgG control.

Proliferative studies of human endothelial progenitors. Following 96 h of culture in RPMI with either 20% normal rat serum, ischemic rat serum or 20 ng/ml VEGF, the proportion of CD117^{Bright}/GATA-2^{Hi} and CD117^{Dim}/GATA-2^{Lo} cells was quantified by flow cytometry and [^{3}H] thymidine (Amersham) (1 μCi/well) uptake measured in an LK Betaplate liquid scintillation counter (Wallace, Gaithersburg, Maryland).

Cell culture and immunocytochemistry. CD34$^+$ cells (> 98% purity) from individual donors were cultured in RPMI with 10% FCS and bovine brain extract (Clonetics, San Diego, California). After culture for 7 d, adherent monolayers were incubated with either 10 μg/ml lipoprotein labeled with the fluorescent probe 1,1-dioctadecyl-3,3,3,3-tetramethyl indocarbocyanine perchlorate (DiI-Ac-LDL) (Molecular Probes, Eugene, Oregon), or with mAbs against CD34, CD31 and factor VIII, and examined by fluorescence microscopy or immunoperoxidase technique.

Animals, surgical procedures and injection of human cells. Rowett (rnu/rnu) athymic nude rats (Sprague–Dawley, Indianapolis, Indiana) were used in studies approved by the Columbia University Institute for Animal Care and Use Committee. After anesthesia, a left thoracotomy was performed, the pericardium was opened and the left anterior descending (LAD) coronary artery was either ligated or left intact (sham procedure). After 48 h, rats were injected in the tail vein with 2.0×10^6 DiI-labeled human CD34$^+$ cells from a single donor. Controls consisted of LAD-ligated rats that were injected with either saline, CD34$^-$ cells or SVEC (Clonetics, San Diego, California). Each group consisted of 6–10 rats.

Analyses of myocardial function. Echocardiographic studies were performed by a blinded investigator (ST) using a high frequency liner array transducer (SONOS 5500, Hewlett Packard, Andover, Massachusetts). Two-dimensional images were obtained at mid-papillary and apical levels. End-diastolic (EDV) and end-systolic (ESV) left ventricular volumes were obtained by bi-plane area-length method and percent left ventricular ejection fraction was calculated as: $[(EDV - ESV) \div EDV] \times 100$. Cardiac output (CO) was measured using an ultrasonic flowprobe (Transonic Systems, Ithaca, New York) and cardiac index was calculated as CO per weight.

Histology and immunohistochemistry. After excision at 2 and 15 wk, left ventricles from each experimental animal were sliced into 10–15 transverse sections from apex to base and representative sections were fixed in formalin and stained for routine histology (H&E) and Masson trichrome stain to evaluate collagen content on a semiquantitative scale (0–3+). The lengths of the infarcted surfaces, involving both epicardial and endocardial regions, were measured with a planimeter digital image analyzer and expressed as a percentage of the total ventricular circumference. Infarct size was expressed as percent of total left ventricular area. In order to quantify capillary density and species origin of the capillaries, additional sections were freshly stained with mAbs against factor VIII, rat or human CD31 (Serotec, Raleigh, North Carolina), and rat or human MHC class I (Accurate Chemicals, Westbury, New York), and counterstained by immunoperoxidase technique (Vector Labs, Burlingame, California). Capillary density was expressed as factor-VIII$^+$ endothelial cells per HPF (×600). All studies were performed by a blinded pathologist (M.J.S.).

Determination of myocyte size. Myocyte size was measured in normal rat hearts and in the infarct zone, peri-infarct rim and distal areas of infarct tissue sections stained by trichrome. The transverse and longitudinal diameters (mm) of 100–200 myocytes in each of 10–15 high-powered fields were measured at ×400 using Image-Pro Plus software.

RT-PCR for human *GATA2*. Poly(A)$^+$ mRNA was extracted by standard methods

from either human CD34$^+$ cells sorted on the basis of CD117 bright or dim expression, or from bone marrow and hearts of normal or infarcted rats receiving either CD34$^+$ or CD34$^-$ cells. RNA extracted from 1×10^6 cells was primed with oligo (dT) 15-mer and random hexamers, and reverse transcribed with Monoley murine lymphotrophic virus reverse transcriptase (Invitrogen, Carlsbad, California). cDNA was amplified for 30 cycles using Taq polymerase (Invitrogen), 3,000 Ci/mmol, [^{32}P]ddATP (Amersham) and primers for human GATA-2 and GAPDH (Fisher Genosys, The Woodlands, Texas). Primer pairs (sense/antisense) for human *GATA2* were AGCCGGCACCTGTTGTGCAA/TGACTTCTCCTGCATGCACT, and for GAPDH were TGAAGGTCGGAGTCAACGGATTTG/CATGTGGGCCATGAGGTCCACCAC. The labeled samples were loaded into 2% agarose gels, separated by electrophoresis, and exposed for radiography for 6 h at –70 °C.

Measurement of myocyte apoptosis by TUNEL assay of paraffin tissue sections. For *in situ* detection of apoptosis at the single-cell level we used the TUNEL assay[36,37] (Boehringer). Rat myocardial tissue sections were obtained from LAD-ligated rats at two wk after injection of either saline or CD34$^+$ human cells, and from healthy rats as negative controls. Briefly, tissues were deparaffinized, digested with Proteinase K and incubated with TdT and fluorescein-labeled dUTP in a humid atmosphere for 60 min at 37 °C. After incubation for 30 min with an antibody specific for fluorescein-conjugated alkaline phosphatase (AP; Boehringer), the TUNEL stain was visualized with a substrate system in which nuclei with DNA fragmentation stained blue (BCIP/NBT substrate system, DAKO, Carpinteria, California). To determine the proportion of apoptotic nuclei within myocytes, tissue was counterstained with a monoclonal antibody specific for desmin (Sigma). Tissue sections were examined microscopically at ×40 magnification and at least 100 cells were counted in a minimum of 8 high-power fields. The percentage of apoptotic myocytes was termed the apoptotic index.

RECEIVED 25 OCTOBER 2000; ACCEPTED 26 FEBRUARY 2001

1. Mahon, N.G. *et al.* Hospital mortality of acute myocardial infarction in the thrombolytic era. *Heart* **81**, 478–482 (1999).
2. Pfeffer, J.M., Pfeffer, M.A., Fletcher, P.J. & Braunwald, E. Progressive ventricular remodeling in rat with myocardial infarction. *Am. J. Physiol.* **260**, H1406–1414 (1991).
3. White, H.D. *et al.* Left ventricular end systolic volume as the major determinant of survival after recovery from myocardial infarction. *Circulation* **76**, 44–51 (1987).
4. Colucci, W.S. Molecular and cellular mechanisms of myocardial failure. *Am. J. Cardiol.* **80**, 15L–25L (1997).
5. Ravichandran, L.V. & Puvanakrishnan, R. *In vivo* labeling studies on the biosynthesis and degradation of collagen in experimental myocardial myocardial infarction. *Biochem. Intl.* **24**, 405–414 (1991).
6. Agocha, A., Lee, H.W. & Eghali-Webb, M. Hypoxia regulates basal and induced DNA synthesis and collagen type I production in human cardiac fibroblasts: effects of TGF-β, thyroid hormone, angiotensis II and basic fibroblast growth factor. *J. Mol. Cell. Cardiol.* **29**, 2233–2244H (1997).
7. Tomita, S. *et al.* Autologous transplantation of bone marrow cells improves damaged heart function. *Circulation* **100**, 247–256 (1999).
8. Liechty, K.W. *et al.* Human mesenchymal stem cells engraft and demonstrate site-specific differentiation after in utero transplantation in sheep. *Nature Med.* **6**, 1282–1286 (2000).
9. Pittenger, M.F. *et al.* Multilineage potential of adult human mesenchymal stem cells. *Science* **284**, 143–147 (1999).
10. Makino, S. *et al.* Cardiomyocytes can be generated from marrow stromal cells *in vitro*. *J. Clin. Invest.* **103**, 697–705 (1999).
11. Nelissen-Vrancken, H., Debets, J., Snoeckx, L., Daemen, M. & Smits, J. Time-related normalization of maximal coronary flow in isolated perfused hearts of rats with myocardial infarction. *Circulation* **93**, 349–355 (1996).
12. Kalkman, E.A.J. *et al.* Determinants of coronary reserve in rats subjected to coronary artery ligation or aortic banding. *Cardiovasc. Res.* **32**, 1088–1095 (1996).
13. Heymans, S. *et al.* Inhibition of plasminogen activators or matrix metalloproteinases prevents cardiac rupture but impairs therapeutic angiogenesis and causes cardiac failure. *Nature Med.* **5**, 1135–1142 (1999).
14. Hochman, J.S. & Choo, H. Limitation of myocardial infarct expansion by reperfusion independent of myocardial salvage. *Circulation* **75**, 299–306 (1987).
15. White, H.D. *et al.* Long-term prognostic importance of patency of the infarct-related coronary artery after thrombolytic therapy for myocardial infarction. *Circulation* **89**, 61–67 (1994).
16. Nidorf, S.M., Siu, S.C., Galambos, G., Weyman, A.E. & Picard, M.H. Benefit of late coronary reperfusion on ventricular morphology and function after myocardial infarction. *J. Am. Coll. Cardiol.* **20**, 307–313 (1992).
17. Folkman, J. Therapeutic angiogenesis in ischemic limbs. *Circulation* **97**, 1108–10 (1998).
18. Asahara, T. *et al.* Isolation of putative progenitor cells for endothelial angiogenesis. *Science* **275**, 964–967 (1997).
19. Takahashi, T. *et al.* Ischemia- and cytokine-induced mobilization of bone marrow-derived endothelial progenitor cells for neovascularization. *Nature Med.* **5**, 434–438 (1999).
20. Kalka, C. *et al.* Transplantation of *ex vivo* expanded endothelial progenitor cells for therapeutic neovascularization. *Proc. Natl. Acad. Sci. USA* **97**, 3422–3427 (2000).
21. Rafii, S. *et al.* Isolation and characterization of human bone marrow microvascular endothelial cells: hematopoietic progenitor cell adhesion. *Blood* **84**, 10–19 (1994).
22. Shi, Q. *et al.* Evidence for circulating bone marrow-derived endothelial cells. *Blood* **92**, 362–367 (1998).
23. Lin, Y., Weisdorf, D.J., Solovey, A. & Hebbel, R.P. Origins of circulating endothelial cells and endothelial outgrowth from blood. *J. Clin. Invest.* **105**, 71–77 (2000).
24. Tavian, M. *et al.* Aorta-associated CD34 hematopoietic cells in the early human embryo. *Blood* **87**, 67–72 (1996).
25. Jaffredo, T., Gautier, R., Eichmann, A. & Dieterlen-Lievre, F. Intraaortic hemopoietic cells are derived from endothelial cells during ontogeny. *Development* **125,** 4575–4583 (1998).
26. Kennedy, M. *et al.* A common precursor for primitive erythropoiesis and definitive haematopoiesis. *Nature* **386**, 488–493 (1997).
27. Choi, K., Kennedy, M., Kazarov, A., Papadimitriou, N. & Keller, G. A common precursor for hematopoietic and endothelial cells. *Development* **125**, 725–732 (1998).
28. Elefanty, A.G., Robb, L., Birner, R. & Begley, C.G. Hematopoietic-specific genes are not induced during *in vitro* differentiation of scl-null embryonic stem cells. *Blood* **90**, 1435–1447 (1997).
29. Labastie, M.C., Cortes, F., Romeo, P.H., Dulac, C. & Peault, B. Molecular identity of hematopoietic precursor cells emerging in the human embryo. *Blood* **92**, 3624–3635 (1998).
30. Tsai, F.Y. *et al.* An early hematopoietic defect in mice lacking the transcription factor GATA-2. *Nature* **371**, 221–225 (1994).
31. Ogawa, M. *et al.* Expression of α_4-integrin defines the earliest precursor of hematopoietic cell lineage diverged from endothelial cells. *Blood* **93**, 1168–1177 (1999).
32. Peichev, M. *et al.* Expression of VEGFR-2 and AC133 by circulating human CD34(+) cells identifies a population of functional endothelial precursors. *Blood* **95**, 952–958 (2000).
33. Asahara, T. *et al.* VEGF contributes to postnatal neovascularization by mobilizing bone marrow-derived endothelial progenitor cells. *EMBO J.* **18**, 3964–3972 (1999).
34. Olivetti, G., Capasso, J.M., Meggs, L.G., Sonnenblick, E.H. & Anversa, P. Cellular basis of chronic ventricular remodeling after myocardial infarction in rats. *Circ. Res.* **68**, 856–869 (1991).
35. Braunwald, E. & Pfeffer, M.A. Ventricular enlargement and remodelling following acute myocardial infarction: mechanisms and management. *Am. J. Cardiol.* **68**, 1–6D (1991).
36. Narula, J. *et al.* Apoptosis in myocytes in end-stage heart failure. *N. Engl. J. Med.* **335**, 1182–1189 (1996).
37. Cheng, W. *et al.* Programmed myocyte cell death affects the viable myocardium after infarction in rats. *Exp. Cell. Res.* **226**, 316–327 (1996).
38. Hart, P.H. *et al.* Activation of human monocytes by granulocyte-macrophage colony-stimulating factor: increased urokinase-type plasminogen activator activity. *Blood* **77**, 841–848 (1991).
39. Stacey, K.J. *et al.* Regulation of urokinase-type plasminogen activator gene transcription by macrophage colony-stimulating factor. *Mol. Cell. Biol.* **15**, 3430–3441 (1995).
40. Pei, X.H. *et al.* G-CSF increases secretion of urokinase-type plasminogen activator by human lung cancer cells. *Clin. Exp. Metastasis* **16**, 551–558 (1998).
41. Dorfman, D.M., Wilson, D.B., Bruns, G.A. & Orkin, S.H. Human transcription factor GATA-2. Evidence for regulation of preproendothelin-1 gene expression in endothelial cells. *J. Biol. Chem.* **267**, 1279–1285 (1992).
42. Ito, H. *et al.* Endothelin-1 is an autocrine/paracrine factor in the mechanism of angiotensin II-induced hypertrophy in cultured rat cardiomyocytes. *J. Clin. Invest.* **92**, 398–403 (1993).
43. Kalkman, E.A.J., van Haren, P., Saxena, P.R. & Schoemaker, R.G. Regionally different vascular response to vasoactive substances in the remodeled infarcted rat heart; aberrant vasculature in the infarct scar. *J. Mol. Cell. Cardiol.* **29**, 1487–1497 (1997).
44. McEwan, P.E., Gray, G.A., Sherry, L., Webb, D.J. & Kenyon, C.J. Differential effects of angiotensin II on cardiac cell proliferation and intramyocardial perivascular fibrosis *in vivo*. *Circulation* **98**, 2765–2773 (1998).
45. Kawano, H. *et al.* Angiotensin II has multiple profibrotic effects in human cardiac fibroblasts. *Circulation* **101**, 1130–1137 (2000).
46. Pfeffer, M.A. *et al.* Effect of captopril on mortality and morbidity in patients with left ventricular dysfunction after myocardial infarction. Results of the survival and ventricular enlargement trial. The SAVE investigators. *N. Engl. J. Med.* 327, 669–677 (1992).
47. The SOLVD investigators. Effect of enalapril on survival in patients with reduced left ventricular ejection fractions and congestive heart failure. *N. Engl. J. Med.* 325, 293–302 (1991).
48. Pitt, B. *et al.* Randomised trial of losartan versus captopril in patients over 65 with heart failure (Evaluation of Losartan in the Elderly Study, ELITE). *Lancet* 349, 747–752 (1997).